JET PROPULSION LABORATORY INTERNAL DOCUMENT

JPL D-19562
September 1, 2000

An Optimization Approach to Orienting Three Spacecraft Reaction Wheel Actuators with Application to the Europa Orbiter

David S. Bayard
Autonomy and Control Section (345)
Jet Propulsion Laboratory
California Institute of Technology
4800 Oak Grove Drive
Pasadena, CA 91109

An Optimization Approach to Orienting Three Spacecraft Reaction Wheel Actuators with Application to the Europa Orbiter

David S. Bayard
Jet Propulsion Laboratory
California Institute of Technology
4800 Oak Grove Drive
Pasadena, CA 91109

ABSTRACT

This report introduces an optimization approach to finding the best way to orient three reaction wheels on an orbiting spacecraft. For this purpose, a quadratic cost function is constructed based on torque, momentum storage, and power requirements. Since momentum management is such an important issue for an orbiting spacecraft, a simple momentum management strategy is also parametrized and included as part of the overall optimization process. The main consideration in this study is to find an orientation which minimizes mass and power of the required reaction wheels, while allowing a specified maximum amount of time between momentum dumps for science acquisition. Several case studies are given to demonstrate convergence of the method, including an application to the NASA/JPL's future Europa orbiter mission. This is a preliminary study which considers the orientation of 3 reaction wheels. A future report will consider the more complex case of orienting 4 reaction wheels.

Contents

1 INTRODUCTION

Reaction wheels are often used as actuators for controlling spacecraft attitude. This report takes an optimization approach to finding the best way to orient three reaction wheels on an orbiting spacecraft. For this purpose, a quadratic cost function is constructed based on torque, momentum storage, and power requirements. Since momentum management is such an important issue for an orbiting spacecraft, a simple momentum management strategy is also parametrized and included as part of the overall optimization process. The main consideration in this study is to find an orientation which minimizes mass and power of the required reaction wheels, while allowing a specified amount of time between momentum dumps.

The approach taken in this paper is to parametrize each reaction wheel with its own unit vector direction. This approach is the most general possible, and avoids imposing a-priori restrictions on wheel geometry. This is in contrast to earlier results which impose a pyramid structure to simplify the problem. For example, the approach in Fleming and Ramos [5] optimizes over the single cant angle associated with a 4-wheel square pyramid configuration, while the approach in Hablani [8] optimizes over the two angles associated with a 4-wheel rectangular pyramid. Although the present analysis considers fewer wheels (3 versus 4) there are a full 6 degrees-of-freedom involved in the optimization problem, compared to only 1 DOF in [5], and 2 DOF in [8]. In principle, the extra degrees of freedom can lead to better performance. Of course, this added performance must be traded against a potentially more complex implementation. Along these same lines, the optimization of 8 DOF associated with a 4-wheel configuration will be considered in a future paper.

The target application for this work is the Europa Orbiter. The Europa Orbiter is part of the NASA's Outer Planets/Solar Probe Project, and is a mission to send a spacecraft to orbit Europa (Jupiter's fourth largest moon) in order to to measure the thickness of the surface ice, and to detect an underlying liquid ocean if it exists.

The Europa Orbiter has tight mass and power limitations. To help reduce wheel mass it is assumed that the wheels are used with their full bipolar capacity, i.e., that zero-rate crossings are acceptable over the course of each orbit. However, this same strategy may not be desirable for other missions with larger mass and power budgets, and/or which may be sensitive to the additional disturbances induced at the zero-crossings.

Mathematically, a QR factorization of the orientation matrix is used to decompose the optimization problem such that rotation matrix Q and skewness matrix R of the wheel frame can be optimized separately. Rotation is optimized analytically (and globally) using a new result given in Appendix A, while the skewness is optimized using a Sequential Quadratic Programming (SQP) approach. Several case studies are given to demonstrate the convergence of method, including an application to the NASA/JPL's emerging Europa orbiter mission.

The report is organized as follows. Background on the reaction wheel orientation problem is given in Section 2, with momentum, torque and power requirements discussed in

Section 3. In Section 4, a cost function is defined for optimization purposes which incorporates requirement-relevant weighting functions. An algorithm for optimization of the cost is given in Section 5, based on a QR factorization of the orientation matrix. The convergence of the algorithm is demonstrated by numerical example for three case studies in Section 6. Conclusions are postponed until Section 7.

Appendices A and B are included to give details behind the Steps 1 and 3, respectively, of the optimization procedure. Appendix C is included for pedagogical reasons, providing a simplified proof for a special case of the result given in Appendix B.

2 BACKGROUND

Let the vector $x_w \in \mathcal{R}^3$ denote a physical quantity (e.g., torque, momentum, etc.) such that the i'th element of x_w is associated with the i'th reaction wheel, $i = 1, 2, 3$. Vectors defined in this manner will be said to be in *wheel coordinates.* The mapping from wheel coordinates to body coordinates is given by the expression,

$$x_b = Ax_w \tag{2.1}$$

$$A = [a_1, a_2, a_3] \tag{2.2}$$

where $A \in \mathcal{R}^{3\times 3}$ denotes a 3×3 **wheel orientation matrix** (with columns a_i, $i = 1, 2, 3$), and x_b is the corresponding vector quantity in spacecraft body coordinates. Physically, the i'th column of the A matrix denotes the orientation of the i'th reaction wheel expressed as a unit vector in body coordinates. Hence the columns of the A matrix are not arbitrary, but are each constrained to have unit norm, i.e.,

$$a_i^T a_i = 1, \quad i = 1, 2, 3 \tag{2.3}$$

Note, however, that in the present treatment, the columns of A are not required to be orthogonal. This permits the reaction wheels to attain (possibly) skewed configurations.

3 REQUIREMENTS

Reaction wheel requirements are most simply stated in terms of an *idealized* set of three reaction wheels which are assumed be oriented along each of the body axes. For example, a simulation can be run which assumes (artificially) that the reaction wheels are oriented along the body axes, to numerically generate the wheel torque and momentum storage requirements. For notational purposes, all quantities associated with such an idealized reaction wheel frame will be denoted with a star $'*'$.

This idealized reaction wheel frame is not necessarily optimal for any criteria. However, requirements specified for wheels in the body frame are easily calculated and visualized, and they can then be mapped, as a separate step, into any other candidate set of reaction wheel coordinates being considered as part of the optimization process.

The baseline scenario (motivated by the Europa orbiter mission) will involve an orbiting spacecraft which accumulates momentum in a nearly repetitive fashion due to periodic orbital dynamics and attitude histories. For example, in the case of the Europa orbiter, the main attitude modes are for nadir pointing and inertially held earth pointing. Because mass is a critical factor in the Europa design, the reaction wheels will be operated in a bipolar fashion, allowing for zero-rate crossings and taking advantage of their full momentum excursion.

3.1 Momentum Requirements

At some starting time $t = 0$, the spacecraft momentum is assumed to be brought (by active management) to a starting momentum "bias" level denoted as b^* (Nms) in idealized reaction wheel coordinates. The idealized reaction wheels then start accumulating momentum over the orbit with both periodic and secular components to give a total stored momentum at time t of $h^*(t)$. It will be convenient to define the momentum accumulated *in excess of* b^* as $\Delta h^*(t)$, so that the total stored momentum can be written as,

$$h^*(t) = b^* + \Delta h^*(t) \tag{3.1}$$

The accumulation of momentum continues until some specified time T (generally a fixed multiple or fraction of the orbital period) at which time the stored momentum is brought back again by active management to its starting bias level of b^*. The process then repeats in this fashion, defining a nominal momentum management strategy over the course of the mission.

It will be convenient to map the momentum bias b^* into wheel coordinates to give the vector b i.e.,

$$b = A^{-1}b^* \tag{3.2}$$

Consider a momentum storage vector $h^*(t) \in \mathcal{R}^3$ at time t in body coordinates which must be attainable using the designed wheel orientation. The momentum vector can be similarly

mapped into wheel coordinates as,

$$h_w(t) = A^{-1}h^*(t) \tag{3.3}$$

It is assumed that all wheels are identical, each with a maximum momentum storage capacity of $\pm\beta$ (Nms). Then conditions which ensure that no wheel is exceeding its maximum storage capacity at time t are given by,

$$-\beta\ \mathit{1} \leq A^{-1}h^*(t) \leq \beta\ \mathit{1} \tag{3.4}$$

where,

$$\mathit{1} \triangleq \begin{bmatrix} 1 \\ 1 \\ 1 \end{bmatrix} \tag{3.5}$$

Note that using (3.1), the $t = 0$ case can be treated separately, and (3.4) can be broken into the two conditions,

$$-\beta\mathit{1} \leq b \leq \beta\mathit{1} \qquad \text{for } t = 0 \tag{3.6}$$

$$-\beta\mathit{1} \leq b + A^{-1}\Delta h^*(t) \leq \beta\mathit{1} \qquad \text{for } 0 < t \leq T \tag{3.7}$$

Constraints (3.6) and (3.7) are functions of b and A and specify the basic momentum requirements in wheel coordinates.

3.2 Torque Requirements

The torque required in body coordinates during this period of time is denoted as the time-varying torque vector $\tau^*(t) \in \mathcal{R}^3$. At each time, the torque vector $\tau^*(t)$ must be attainable using the designed wheel orientation. The torque vector can be mapped into wheel coordinates as,

$$\tau_w(t) = A^{-1}\tau^*(t) \tag{3.8}$$

where $\tau_w(t) \in \mathcal{R}^3$ denotes the torque vector in wheel coordinates. It is assumed that all wheels are identical, each with maximum torque capability of $\pm\gamma$ (Nm). Then the condition which ensures that no wheel is exceeding its maximum torque capacity at time t is given by,

$$-\gamma\mathit{1} \leq A^{-1}\tau^*(t) \leq \gamma\mathit{1} \tag{3.9}$$

Constraint (3.9) is a function of A and specifies the basic torque requirements in wheel coordinates.

3.3 Power Requirements

Let the total power expended due to reaction wheels at time t associated with a specific wheel configuration be denoted by $P(t)$. The power dissipated $P(t)$ will be assumed to be approximated by the model $P_1(t)$ defined as,

$$P_1(t) = p_0 + \alpha ||w(t)||_1 \tag{3.10}$$

where the wheel speed vector $w(t) = [w_1(t), w_2(t), w_3(t)]^T$ has components $w_i(t)$ which correspond to the speed of the i'th wheel, and $||\cdot||_1$ denotes the standard L_1 vector norm,

$$||w(t)||_1 = \sum_{i=1}^{3} |w_i(t)| \tag{3.11}$$

The constant p_0 in (3.10) accounts for power loss in the electronics and other fixed dissipative effects. The wheel rate term $w(t)$ captures long term dissipation effects associated with countering frictional torques. The value for α is best obtained by fitting empirical data. The angular acceleration $\dot{w}$ is intentionally omitted from this model since it is not a major contributor to long-term power dissipation issues. However, it is important for calculating peak-power requirements (e.g., during maneuvers) and should be checked against the final design.

For optimization purposes, the P_1 power model (3.10) will be replaced by the P_2 model given below,

$$P_2(t) = p_0 + \alpha ||w(t)||_2 \tag{3.12}$$

where $||\cdot||_2$ denotes the standard L_2 (Euclidean) vector norm,

$$||w(t)||_2 = \left(\sum_{i=1}^{3} |w_i(t)|^2 \right)^{\frac{1}{2}} \tag{3.13}$$

The P_2 model (3.12) only approximates the P_1 model, but has the advantage of leading to a more tractable optimization problem. The L_1 norm can be bounded on either side by the L_2 norm as [7],

$$||w(t)||_2 \leq ||w(t)||_1 \leq \sqrt{2} \cdot ||w(t)||_2 \tag{3.14}$$

Hence, the minimization of P_2 power indirectly acts to minimize P_1 power to within a factor of $\sqrt{2}$. Numerical results indicate that this approximate approach can be very effective.

It is known that the wheel speed is proportional to the wheel momentum, i.e.,

$$I_w w(t) = h_w(t) = A^{-1} h^*(t) \tag{3.15}$$

where I_w $(Kg\ m^2)$ is a scalar value for the individual wheel inertia (assumed to be the same for all wheels). Using (3.15), the P_2 power model (3.12) can be rewritten as,

$$P_2(t) = p_0 + \frac{\alpha}{I_w} ||A^{-1} h^*(t)||_2 \tag{3.16}$$

The condition for power $P_2(t)$ to be less than some desired specified value P_d is then given by,

$$||A^{-1}h^*(t)||_2 \leq \frac{\overline{p}\ I_w}{\alpha} \tag{3.17}$$

where $\overline{p} = P_d - p_0$. As done for the momentum, the $t = 0$ case can be broken out separately to give the two constraints,

$$||b||_2 \leq \frac{\overline{p}\ I_w}{\alpha}, \quad \text{for } t = 0 \tag{3.18}$$

$$||b + A^{-1}\Delta h^*(t)||_2 \leq \frac{\overline{p}\ I_w}{\alpha}, \quad \text{for } 0 < t \leq T \tag{3.19}$$

Constraints (3.18) and (3.19) are functions of b and A and specify the basic power requirements.

3.4 Discussion

A *feasible design* of b and A is defined as one which meets the momentum storage requirements (3.6)(3.7), torque requirements (3.9), and power requirements (3.18)(3.19). The present approach will be to optimize a certain cost function which tends to drive b and A towards a feasible design. The cost function is discussed in the next section.

As one practical use of the optimization tool, the mass and/or power of the specified wheels can be systematically reduced until a feasible solution is no longer obtained. This establishes a bound on the smallest set of wheels which are capable of doing the job, and is useful for sizing and understanding wheel requirements.

4 COST FUNCTION

The optimization problem will focus on a specific discrete set of times t_k, $k = 1, ..., n$. At each time t_k, let the desired torque be given as $\tau^*(k)$ and the excess accumulated momentum be given as $\Delta h^*(k)$. Here, the t dependence has been replaced by k for notational simplicity, since the set of constraint times is now finite.

The goal is to optimize a cost function $C(b, A)$ over the choice of both the initial bias momentum b and the reaction wheel orientation A, i.e.,

$$\min_{b,A} \; C(b, A) \tag{4.1}$$

The cost function is taken to be the sum of three components:

$$C(b, A) = C_M + C_T + C_P \tag{4.2}$$

where each component is defined below.

Momentum Cost Function

$$C_M(b, A) = \frac{1}{\beta^2} \left(||b||_2^2 + \sum_{k=1}^{n} ||b + A^{-1}\Delta h^*(k)||_2^2 \right) \tag{4.3}$$

Torque Cost Function

$$C_T(b, A) = \frac{1}{\gamma^2} \sum_{k=1}^{n} ||A^{-1}\tau^*(k)||_2^2 \tag{4.4}$$

Power Cost Function

$$C_P(b, A) = \frac{\alpha^2}{\bar{p}^2 \; I_w^2} \left(||b||_2^2 + \sum_{k=1}^{n} ||b + A^{-1}\Delta h^*(k)||_2^2 \right) \tag{4.5}$$

The cost function (4.2) is a weighted sum of L_2 norms (i.e,. weighted least squares criteria) where the weightings are chosen to normalize the importance of each term according to their specified requirements. For example, the $\frac{1}{\beta^2}$ weighting associated with C_M cost in (4.3) is motivated by the need to satisfy the momentum storage requirements given in (3.6)(3.7). Similarly the scalings for C_T and C_P above are motivated by the need to satisfy the torque requirements (3.9), and power requirements (3.18)(3.19), respectively. The advantage of these scalings is that they transform the cost into dimensionless units, which acts to drive each of the quantities to satisfy their desired constraints. This overcomes the usual difficulty of scaling costs in problems with multiple objectives.

Numerical values for $\beta, \gamma, \alpha, \overline{p}, I_\omega$ are needed to properly scale the optimization problem. In practice, these parameters can be chosen based on a nominal reaction wheel design. The use of the L_2 norm here is largely motivated by mathematical convenience to lead to a reasonably tractable solution, and is not the same as enforcing strict satisfaction of constraints using a weighted L_∞ norm. The possibility of L_∞ norm optimization is left as a topic for future investigation.

The choice of times t_k at which to enforce the constraints is left up to the designer. In practice, these constraints can be specified in several ways,

1. by discretizing time over a grid, and specifying momentum and torque constraints (in the idealized star frame) based on an actual simulation of the spacecraft in orbit
2. by choosing times of maximum excursions of the momentum and torque (in the idealized star frame), as generated by a simulation of the spacecraft in orbit
3. by not interpreting t_k as time directly, but by using k as an index to define a set of linear constraints forming a simplex which overbounds the region (in the idealized star frame) containing all simulated momentum and torque values.
4. As a special case of the last item, where one uses the eight corners of a box aligned with the body axes to specify the constraints associated with the idealized star frame.

Any one of these choices can be used with the optimization approach presented subsequently. For simplicity, the last choice will be used for the final implementation. Similar formulations making use of torque boxes and momentum cylinders have appeared in the literature [4][8].

5 OPTIMIZATION PROCEDURE

5.1 Parametrization of Orientation Matrix

It will be convenient for optimization purposes to represent the matrix A in terms of its QR factors (cf., [7]), i.e.,

$$A = QR \tag{5.1}$$

where $Q \in \mathcal{R}^{3\times 3}$ is an orthogonal matrix (i.e., $QQ^T = Q^TQ = I$) and R is an upper triangular matrix. Intuitively, the R matrix represents the skewness of the wheel coordinate frame, and the Q matrix represents any rotations and/or reflections.

By the orthogonality of Q the unit norm constraints (2.3) on the columns of A become unit norm constraints on the columns of R. Hence, R is upper triangular with unit norm columns. Accordingly, it will be parametrized as follows,

$$R = \begin{bmatrix} 1 & a & c \\ 0 & (1-a^2)^{\frac{1}{2}} & b(1-c^2)^{\frac{1}{2}} \\ 0 & 0 & (1-b^2)^{\frac{1}{2}}(1-c^2)^{\frac{1}{2}} \end{bmatrix} \tag{5.2}$$

It can be verified that the columns of R are unit norm by construction. Specifically, the second column of R parametrizes all unit vectors in $\mathcal{R}^2$ since with the change of variable $a = \sin(\phi)$ it corresponds to the polar representation $x = \sin(\phi)$, $y = \cos(\phi)$ of the unit circle. Similarly, the last column of R spans all unit vectors in $\mathcal{R}^3$ since with the change of variables $c = \cos(\theta_1)$, $b = \cos(\theta_2)$, it corresponds to the spherical coordinate representation $x = \cos(\theta_1)$, $y = \cos(\theta_2)\cos(\theta_1)$ and $z = \cos(\theta_2)\cos(\theta_1)$ of the unit sphere.

In order to prevent the square-root terms in R from becoming imaginary, it will be convenient to impose the following linear constraints,

$$\begin{aligned} -1 &\leq a \leq 1 \\ -1 &\leq b \leq 1 \\ -1 &\leq c \leq 1 \end{aligned} \tag{5.3}$$

Without loss of generality, the square roots in the definition of R (5.2) can always be taken as positive. To prove this assertion, assume that some square root terms are not positive in an arbitrary matrix R^o of the form (5.2). Because individual wheel characteristics are symmetric with respect to polarity, any column of R^o can be multiplied by -1 without changing the value of the cost function. Assume that this is done to make the diagonals of R^o all positive, calling the resulting matrix R^a. Since the diagonal elements of R^a are positive, they can be realized by interpreting their square-roots as positive (as desired). The remaining off-diagonal

elements of R^a can be accommodated within the positive square-root convention by choosing signs of a, b, c appropriately within the linear constraints (5.3)). Hence, an arbitrary R^o can always be written as an equivalent R^a in the form of (5.2) with a, b, c satisfying (5.3) when the square-roots taken as positive.

In all future reference, the notation a, b, c in the expression for R above will be dropped and replaced by the more compact parameter vector notation r where,

$$r = \begin{bmatrix} r_1 \\ r_2 \\ r_3 \end{bmatrix} \triangleq \begin{bmatrix} a \\ b \\ c \end{bmatrix} \tag{5.4}$$

5.2 Three Wheel Optimization Algorithm

Using the QR factorization of A, the cost function (4.2)-(4.5) can be rewritten as,

$$C(b, R, Q) = \frac{1}{c^2}||b||_2^2 + \frac{1}{c^2}\sum_{k=1}^{n}||b + R^{-1}Q^T\Delta h^*(k)||_2^2 + \frac{1}{\gamma^2}\sum_{k=1}^{n}||R^{-1}Q^T\tau^*(k)||_2^2 \tag{5.5}$$

where,

$$\frac{1}{c^2} = \frac{1}{\beta^2} + \frac{\alpha^2}{\overline{p}^2\, I_w^2} \tag{5.6}$$

subject to Q orthogonal, and R upper triangular with unit norm columns.

The basic approach to minimizing $C(b, R, Q)$ is outlined in the following sequence of steps.

Step 0: Initialize

$$\widehat{Q} = I \tag{5.7}$$

Step 1: Optimize over b, R

$$\widehat{b}, \widehat{R} = \arg\min_{b,R}\ C(b, R, \widehat{Q}) \tag{5.8}$$

subject to R upper triangular with unit norm columns.

Step 2:

Calculate the bias in body frame $\widehat{b}^*$

$$\widehat{b}^* = \widehat{Q}\widehat{R}\widehat{b} \tag{5.9}$$

Step 3: Optimize over Q

$$\widehat{Q} = \arg\min_{Q} \; C(\widehat{R}^{-1}Q^T\widehat{b}^*, \widehat{R}, Q) \tag{5.10}$$

subject to Q being an orthogonal matrix i.e., $Q^TQ = I$.

Step 4: Repeat

Repeat Steps 1 to 3 until convergence is obtained.

5.3 Discussion

In Step 1, the optimization is performed using Sequential Quadratic Programming (SQP), and is detailed in Appendix A. It is worth noting that Step 1 is equivalent to,

$$\widehat{b}^*, \widehat{R} = \arg\min_{b^*,R} \; C(R^{-1}\widehat{Q}^Tb^*, R, \widehat{Q}) \tag{5.11}$$

where it is emphasized that this optimization is equivalently taken over the optimal bias momentum in *body frame coordinates* b^*. This fact is important for conceptual reasons discussed below. However, for the actual numerical optimization, it is more convenient to use the bias momentum b in *reaction wheel coordinates* since it is b and not b^* that appears linearly inside the various norm terms of C.

In Step 2, the calculation of the momentum bias in body frame $\widehat{b}^*$ is made for explicit use in the expression (5.10) which keeps it invariant during optimization of Q in Step 3.

In Step 3, the optimization over Q is performed using a globally optimal analytical solution derived in Appendix B.

Together, the optimization in (5.11) and (5.10) (equivalently, Steps 1 and 3) constitute alternating minimizations between the two *independent* parameter sets $\{b^*, R\}$ and $\{Q\}$. This *relaxation* type approach ensures that the algorithm gives a sequence of solutions with a monotonically decreasing cost. Since the cost is bounded below (by zero), the cost converges. Hence the algorithm is convergent in the sense of the cost.

Although the cost converges, the converged solution is not necessarily the globally optimal solution to the original problem, nor is it (in general) even the locally optimal solution which would be obtained by setting the cost gradient to zero. Rather, the main motivation for this approach is to take advantage of a new result in Appendix B which provides a closed-form analytical solution to the subproblem of optimizing over Q. Empirically, this tends to stabilize the overall approach and lead to globally useful solutions. If local optimality is desired, the converged solution can be further iterated using a gradient algorithm. While potentially useful, the additional gradient iteration was not found necessary in the numerical examples studied.

6 NUMERICAL RESULTS

Three case studies are given in this section to demonstrate the use of the algorithm in Section 5.2 for optimizing reaction wheel orientations. The three case studies correspond to an intentional elongation of the momentum and torque requirement boxes in the x direction (Case 1), the y direction (Case 2), and the z direction (Case 3). Case 2 is based on requirements for the Europa orbiter.

6.1 Nominal Wheel Characteristics

A nominal set of three identical reaction wheels is chosen with characteristics given below. These numbers are consistent with a recent Europa mission concept.

```
Individual wheel inertia
Iw=.0509305 (Kg-m^2)
Max individual wheel momentum storage capacity
beta=8 (Nms)
Max single wheel torque capability
gamma=.02 (Nm)
Power dissipation scale factor
alpha=.025 watt/(rad/sec)
```

6.2 Initial Configuration

```
INITIAL DESIGN
RWA Alignment Matrix: Ahat0
     1     0     0
     0     1     0
     0     0     1
Skewness Matrix: Rhat0
     1     0     0
     0     1     0
     0     0     1
Rotation Matrix: Qhat0
     1     0     0
     0     1     0
     0     0     1
bias (in body): bs0
     0
     0
     0
```

6.3 Case 1: X Axis Emphasis

The momentum, torque and power constraints for this case are specified below. The momentum and torque boxes are somewhat exaggerated in the X direction to study the effect of increased requirements along the x-axis.

```
Momentum Box x,y,z (Nms)
        X      Y      Z
Max     5      1      2
Min     0     -1     -2

Torque Box x,y,z (Nm)
            X              Y              Z
Max   2.0000e-002  4.0000e-003  8.0000e-003
Min  -2.0000e-002 -4.0000e-003 -8.0000e-003

Total power allocation-pbar (watts)
  3.1500e+001
```

The iterative algorithm gives a sequence of solutions having the costs given below.

```
************************************************************
Itrn    Cost           Max Momentum  Max Torque    Max Power
------------------------------------------------------------
Allocation:            8.0000e+000   2.0000e-002   3.1500e+001
------------------------------------------------------------
0       1.1821e+001    5.0000e+000   2.0000e-002   3.9269e+000
1       1.0970e+001    4.6755e+000   1.8756e-002   4.3011e+000
2       8.4817e+000    3.5471e+000   1.6890e-002   2.7309e+000
3       8.3114e+000    3.5137e+000   1.7284e-002   2.7330e+000
4       8.2945e+000    5.2380e+000   1.7214e-002   4.7983e+000
5       8.2921e+000    5.2060e+000   1.7122e-002   4.7529e+000
6       8.2907e+000    3.4468e+000   1.7209e-002   2.8186e+000
7       8.2897e+000    5.1984e+000   1.7292e-002   4.7948e+000
8       8.2892e+000    3.4418e+000   1.7348e-002   2.8094e+000
9       8.2889e+000    3.4345e+000   1.7385e-002   2.8017e+000
10      8.2886e+000    3.4245e+000   1.7406e-002   2.7917e+000
11      8.2884e+000    3.4116e+000   1.7413e-002   2.7801e+000
12      8.2883e+000    3.3986e+000   1.7409e-002   2.7680e+000
13      8.2882e+000    3.3854e+000   1.7398e-002   2.7556e+000
14      8.2881e+000    3.3721e+000   1.7382e-002   2.7434e+000
15      8.2880e+000    3.3588e+000   1.7362e-002   2.7311e+000
16      8.2879e+000    3.3457e+000   1.7339e-002   2.7191e+000
17      8.2878e+000    3.3335e+000   1.7317e-002   2.7070e+000
18      8.2876e+000    5.3249e+000   1.7294e-002   4.8936e+000
```

```
19      8.2875e+000   5.3242e+000   1.7272e-002   4.8928e+000
20      8.2874e+000   3.3027e+000   1.7252e-002   2.6782e+000
21      8.2873e+000   3.2943e+000   1.7232e-002   2.6702e+000
22      8.2872e+000   3.2866e+000   1.7213e-002   2.6630e+000
23      8.2871e+000   3.2797e+000   1.7196e-002   2.6564e+000
24      8.2870e+000   3.2734e+000   1.7179e-002   2.6505e+000
25      8.2869e+000   3.2678e+000   1.7164e-002   2.6451e+000
26      8.2868e+000   3.2626e+000   1.7150e-002   2.6406e+000
27      8.2868e+000   3.2580e+000   1.7137e-002   2.6375e+000
28      8.2867e+000   3.2537e+000   1.7125e-002   2.6347e+000
29      8.2867e+000   3.2499e+000   1.7114e-002   2.6322e+000
30      8.2866e+000   3.2464e+000   1.7104e-002   2.6298e+000

Percent Skewness is 24
```

The final optimized solution is given below.

```
************************************************************
FINAL OPTIMIZED VALUES
RWA Alignment Matrix: Ahat
 -8.2916e-001 -5.9268e-001  -8.6391e-001
  4.2622e-001  7.5580e-002  -4.6093e-001
 -3.6170e-001  8.0188e-001  -2.0298e-001

Skewness Matrix: Rhat
  1.0000e+000  2.3361e-001  5.9329e-001
            0  9.7233e-001  1.8084e-001
            0            0  7.8442e-001

Rotation Matrix: Qhat
 -8.2916e-001 -4.1034e-001 -3.7962e-001
  4.2622e-001 -2.4670e-002 -9.0428e-001
 -3.6170e-001  9.1160e-001 -1.9535e-001

momentum bias (in body)
 -2.2221e+000
  3.8240e-005
  4.1523e-005
```

As expected, the strong projections [-8.2916e-001,-5.9268e-001 -8.6391e-001] in the first row of $\widehat{A}$ indicate that the x axis is favored by the optimized wheel configuration. As an intuition check, the optimized momentum bias is seen to be close to the values [-2.5,0,0], which center the momentum box about zero.

The optimized configuration is depicted graphically in Figure 6.1. For visualization pur-

poses, the wheels have been flipped so that each wheel has its largest projection in the positive octant, i.e.,

$$\begin{bmatrix} 8.2916e-001 & -5.9268e-001 & 8.6391e-001 \\ -4.2622e-001 & 7.5580e-002 & 4.6093e-001 \\ 3.6170e-001 & 8.0188e-001 & 2.0298e-001 \end{bmatrix} \tag{6.1}$$

This is possible since each reaction wheel has symmetric behaviour and any column of $\hat{A}$ can be changed in sign without effecting the overall cost. However, Figure 6.1 is only for visualization purposes, and may or may not correspond to the most natural polarities for mounting the reaction wheels on the actual spacecraft.

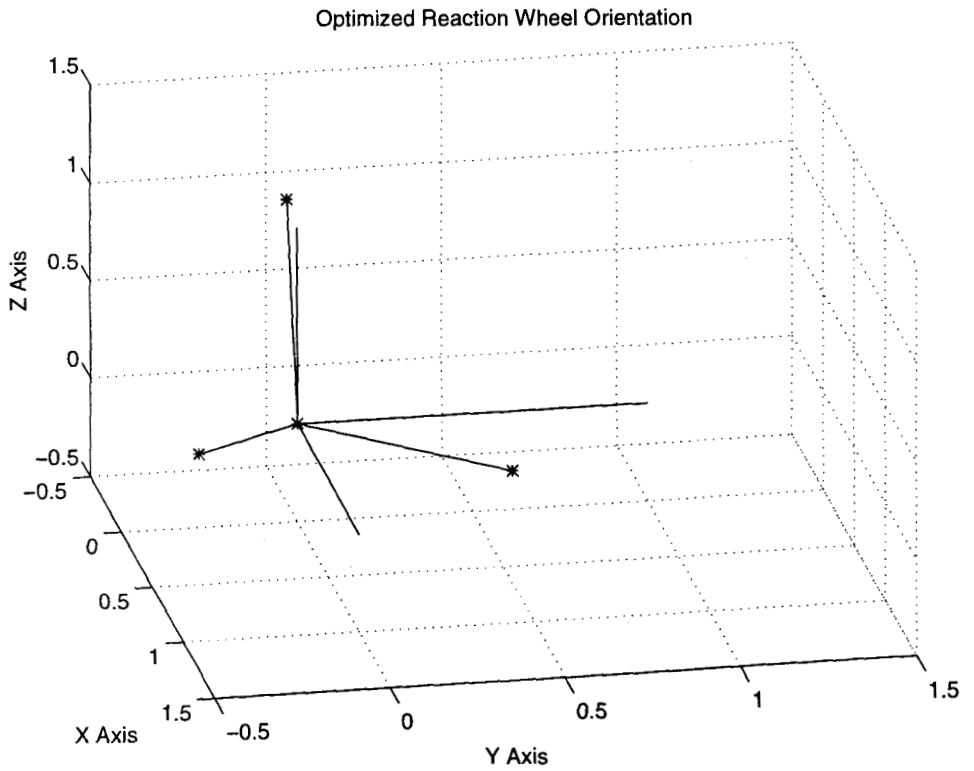

Figure 6.1: Optimized Reaction Wheel Orientation for Case 1

6.4 Case 2: Y Axis Emphasis

The momentum, torque and power constraints for this case are specified below, and correspond to requirements for the Europa orbiter based on preliminary modeling results. The requirements are more stringent in the Y axis because it corresponds to the orbit normal direction.

```
Momentum Box x,y,z (Nms)
            X             Y             Z
Max    3.4300e+000  3.8000e-003  6.9700e+000
Min   -2.2200e-001 -4.9800e+000  2.9400e+000

Torque Box x,y,z (Nm)
            X             Y             Z
Max    1.7700e-003  1.7500e-003  1.4000e-003
Min   -1.7200e-003 -9.8600e-003 -4.8500e-004

Total power allocation-pbar (watts)
  3.1500e+001
```

The iterative algorithm gives a sequence of solutions having the costs given below. It can be seen that the cost may occasionally increase (i.e., only in the 5th significant figure) as the iterations progress. This is partly due to numerical roundoff errors and partly due to the SQP step which is intentionally not run to full completion in the earlier iterations to save on computation.

```
************************************************************
Itrn    Cost           Max Momentum  Max Torque    Max Power
------------------------------------------------------------
Allocation:            8.0000e+000   2.0000e-002   3.1500e+001
------------------------------------------------------------
0       7.0418e+000    6.9700e+000   9.8600e-003   7.5495e+000
1       3.1403e+000    1.0241e+001   8.2358e-003   9.2542e+000
2       3.0414e+000    4.0107e+000   7.5552e-003   3.9294e+000
3       3.0391e+000    4.1244e+000   7.5472e-003   4.0156e+000
4       3.0383e+000    1.2227e+001   7.2696e-003   1.0930e+001
5       3.0382e+000    1.2679e+001   7.5636e-003   1.0374e+001
6       3.0380e+000    4.5789e+000   7.5727e-003   3.6050e+000
7       3.0381e+000    4.6778e+000   7.5934e-003   3.4403e+000
8       3.0381e+000    4.7410e+000   7.6086e-003   3.2931e+000
9       3.0382e+000    4.7864e+000   7.6252e-003   3.1840e+000
10      3.0383e+000    1.2523e+001   7.5618e-003   8.8774e+000
11      3.0384e+000    4.7513e+000   7.5439e-003   3.1516e+000
12      3.0384e+000    4.7637e+000   7.5795e-003   3.1176e+000
13      3.0385e+000    4.7712e+000   7.6012e-003   3.1090e+000
```

```
14      3.0385e+000   4.7789e+000   7.6195e-003   3.1315e+000
15      3.0385e+000   4.7844e+000   7.6347e-003   3.1502e+000
16      3.0385e+000   4.7869e+000   7.6430e-003   3.1648e+000
17      3.0385e+000   4.7895e+000   7.6438e-003   3.1708e+000
18      3.0383e+000   4.7951e+000   7.6405e-003   3.1676e+000
19      3.0382e+000   4.8030e+000   7.6359e-003   3.1592e+000
20      3.0381e+000   4.8112e+000   7.6306e-003   3.1492e+000
21      3.0380e+000   4.8193e+000   7.6240e-003   3.1380e+000
22      3.0379e+000   4.8281e+000   7.6181e-003   3.1259e+000
23      3.0378e+000   4.8359e+000   7.6125e-003   3.1147e+000
24      3.0377e+000   4.8431e+000   7.6074e-003   3.1196e+000
25      3.0376e+000   4.8496e+000   7.6026e-003   3.1255e+000
26      3.0376e+000   4.8555e+000   7.5980e-003   3.1311e+000
27      3.0375e+000   4.8610e+000   7.5938e-003   3.1364e+000
28      3.0375e+000   4.8660e+000   7.5898e-003   3.1414e+000
29      3.0374e+000   4.8707e+000   7.5861e-003   3.1461e+000
30      3.0374e+000   4.8750e+000   7.5826e-003   3.1506e+000

Percent Skewness is  6
```

The final optimized solution is given below.

```
************************************************************
FINAL OPTIMIZED VALUES
RWA Alignment Matrix: Ahat
 -5.8700e-001 -2.8918e-001  5.3041e-001
 -8.0345e-001  2.3296e-001 -8.0643e-001
  9.9452e-002 -9.2850e-001 -2.6143e-001

Skewness Matrix: Rhat
  1.0000e+000 -1.0976e-001  3.1057e-001
            0  9.9396e-001 -6.4812e-002
            0            0  9.4834e-001

Rotation Matrix: Qhat
 -5.8700e-001 -3.5576e-001  7.2723e-001
 -8.0345e-001  1.4565e-001 -5.7728e-001
  9.9452e-002 -9.2316e-001 -3.7133e-001

momentum bias (in body)
 -1.4257e+000
  2.2116e+000
 -4.4042e+000
```

As expected, the strong projections [-8.0345e-001,2.3296e-001,-8.0643e-001] in the second row of $\widehat{A}$ indicate that the y axis is favored by the optimized wheel configuration. As an intuition check, the optimized momentum bias is seen to be close to the values [-1.6040,2.4881,-4.9550] which center the momentum box about zero.

The optimized configuration is depicted graphically in Figure 6.2. For this purpose, wheels are flipped such that each wheel has its largest projection in the positive octant, i.e.,

$$\begin{bmatrix} 5.8700e-001 & 2.8918e-001 & -5.3041e-001 \\ 8.0345e-001 & -2.3296e-001 & 8.0643e-001 \\ -9.9452e-002 & 9.2850e-001 & 2.6143e-001 \end{bmatrix} \tag{6.2}$$

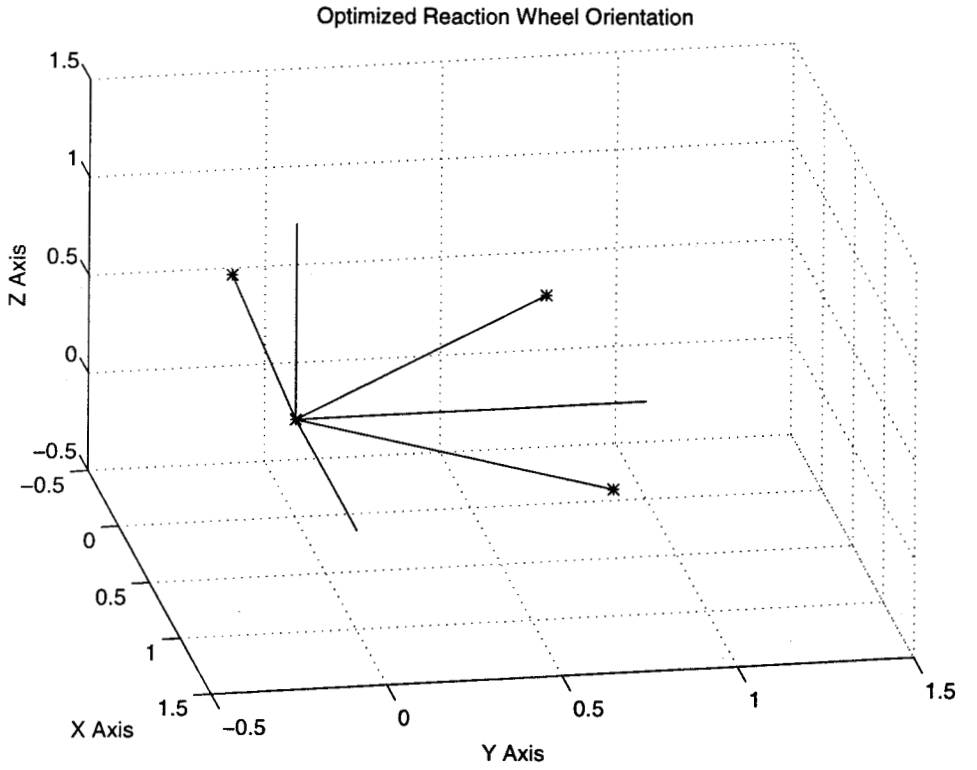

Figure 6.2: Optimized Reaction Wheel Orientation for Case 2

6.5 Case 3: Z Axis Emphasis

The momentum, torque and power constraints for this case are specified below. The momentum and torque boxes are somewhat exaggerated in the Z direction to study the effect of increased requirements along the z-axis.

```
Momentum Box x,y,z (Nms)
            X      Y      Z
Max         1      2      5
Min        -1     -2      0

Torque Box x,y,z (Nm)
            X              Y              Z
Max   4.0000e-003  8.0000e-003  2.0000e-002
Min  -4.0000e-003 -8.0000e-003 -2.0000e-002

Total power allocation-pbar (watts)
  3.1500e+001
```

```
************************************************************
Itrn    Cost           Max Momentum  Max Torque    Max Power
------------------------------------------------------------
Allocation:            8.0000e+000   2.0000e-002   3.1500e+001
------------------------------------------------------------
0       1.1821e+001    5.0000e+000   2.0000e-002   3.9269e+000
1       1.0970e+001    4.7095e+000   1.8749e-002   3.3781e+000
2       8.4892e+000    5.2085e+000   1.6900e-002   4.9720e+000
3       8.3129e+000    5.1203e+000   1.7273e-002   4.8529e+000
4       8.2942e+000    3.4438e+000   1.7212e-002   2.7962e+000
5       8.2916e+000    5.2035e+000   1.7120e-002   4.7480e+000
6       8.2910e+000    5.1626e+000   1.7213e-002   4.7762e+000
7       8.2893e+000    3.4501e+000   1.7298e-002   2.8175e+000
8       8.2897e+000    3.4403e+000   1.7353e-002   2.8094e+000
9       8.2885e+000    3.4349e+000   1.7389e-002   2.7996e+000
10      8.2890e+000    3.4221e+000   1.7408e-002   2.7914e+000
11      8.2882e+000    3.4103e+000   1.7413e-002   2.7774e+000
12      8.2885e+000    3.3963e+000   1.7408e-002   2.7671e+000
13      8.2881e+000    3.3835e+000   1.7396e-002   2.7529e+000
14      8.2882e+000    3.3697e+000   1.7379e-002   2.7420e+000
15      8.2880e+000    3.3565e+000   1.7358e-002   2.7286e+000
16      8.2880e+000    3.3434e+000   1.7335e-002   2.7171e+000
17      8.2878e+000    3.3312e+000   1.7312e-002   2.7047e+000
18      8.2877e+000    5.3248e+000   1.7290e-002   4.8940e+000
19      8.2875e+000    3.3099e+000   1.7268e-002   2.6848e+000
```

```
20      8.2874e+000   3.3007e+000   1.7247e-002   2.6763e+000
21      8.2873e+000   3.2923e+000   1.7227e-002   2.6684e+000
22      8.2872e+000   3.2847e+000   1.7208e-002   2.6612e+000
23      8.2871e+000   3.2779e+000   1.7191e-002   2.6547e+000
24      8.2870e+000   3.2717e+000   1.7175e-002   2.6488e+000
25      8.2869e+000   3.2661e+000   1.7160e-002   2.6435e+000
26      8.2868e+000   3.2610e+000   1.7146e-002   2.6393e+000
27      8.2868e+000   3.2564e+000   1.7133e-002   2.6363e+000
28      8.2867e+000   3.2522e+000   1.7121e-002   2.6335e+000
29      8.2867e+000   3.2484e+000   1.7110e-002   2.6310e+000
30      8.2866e+000   3.2450e+000   1.7100e-002   2.6287e+000

Percent Skewness is 24
```

The final optimized solution is given below

```
************************************************************
FINAL OPTIMIZED VALUES
RWA Alignment Matrix: Ahat
 -4.2652e-001 -7.4669e-002  4.6079e-001
 -3.6065e-001  8.0214e-001 -2.0385e-001
 -8.2946e-001 -5.9245e-001 -8.6378e-001

Skewness Matrix: Rhat
  1.0000e+000  2.3397e-001  5.9346e-001
            0  9.7224e-001  1.7997e-001
            0            0  7.8448e-001

Rotation Matrix: Qhat
 -4.2652e-001  2.5841e-002  9.0411e-001
 -3.6065e-001  9.1183e-001 -1.9620e-001
 -8.2946e-001 -4.0975e-001 -3.7959e-001

momentum bias (in body)
 -3.7899e-005
  4.1385e-005
 -2.2221e+000
```

As expected, the strong projections [-8.2946e-001,-5.9245e-001,-8.6378e-001] in the third row of $\widehat{A}$ indicate that the z axis is favored by the optimized wheel configuration. As an intuition check, the optimized momentum bias is seen to be close to the values [0,0,-2.5] which center the momentum box about zero.

The optimized configuration is depicted graphically in Figure 6.3. For this purpose, wheels

are flipped such that each wheel has its largest projection in the positive octant, i.e.,

$$\begin{bmatrix} 4.2652e-001 & -7.4669e-002 & -4.6079e-001 \\ 3.6065e-001 & 8.0214e-001 & 2.0385e-001 \\ 8.2946e-001 & -5.9245e-001 & 8.6378e-001 \end{bmatrix} \tag{6.3}$$

As a check on the algorithm, this Case 3 has been intentionally designed to be identical to Case 1 under a relabeling of the axes. It can be seen by comparing Case 3 to Case 1 that (within numerical error) the optimized solutions agree.

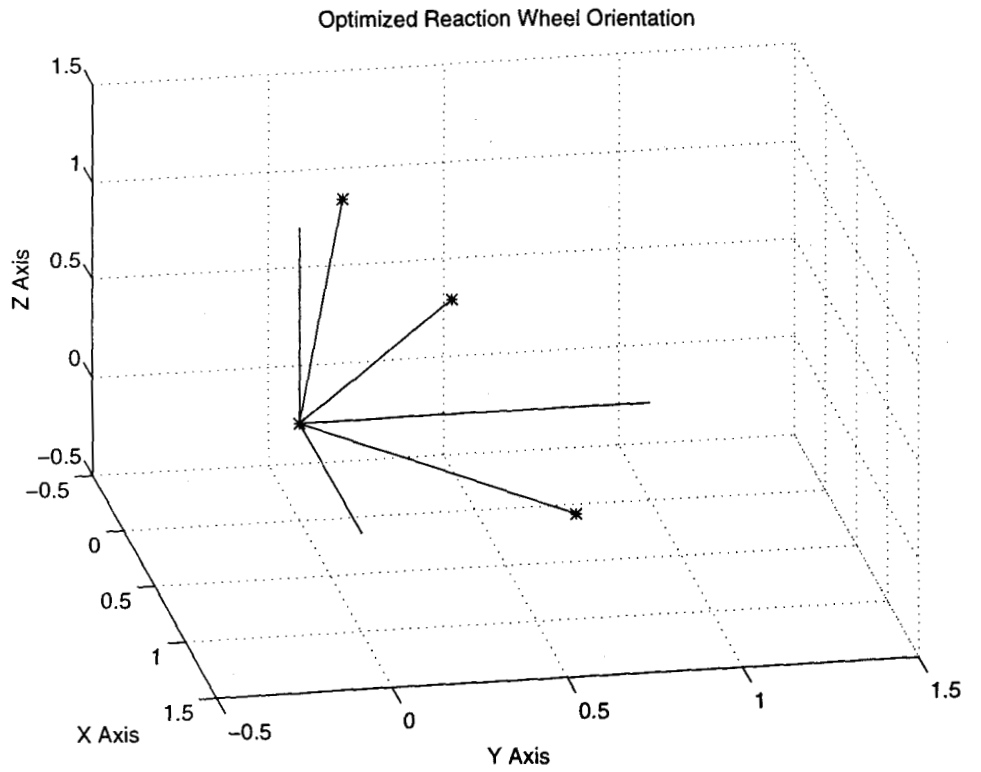

Figure 6.3: Optimized Reaction Wheel Orientation for Case 3

7 CONCLUSIONS

This report has developed an optimization-based approach to orienting three reaction wheels on an orbiting spacecraft. The main consideration has been to find an orientation matrix which minimizes mass and power of the required reaction wheels, while allowing a specified maximum amount of time between momentum dumps.

The optimization is nonlinear in both the cost and constraints. A QR factorization of the wheel-to-body transformation allows separate optimization over the rotation Q and skewness R of the reaction wheel frame. The initial momentum bias b is also optimized for momentum management purposes. The optimization over the Q matrix is performed analytically, while the R, b parameters are optimized using Sequential Quadratic Programming (SQP).

Several case studies were given to demonstrate convergence and performance of the method, including an application to the NASA/JPL's emerging Europa orbiter mission. In each case, the per-wheel requirements are seen to be systematically reduced with continued iteration of the algorithm. The final optimized orientations appear intuitively reasonable, tending to favor the body axis having the most stringent requirements.

The present study considers the orientation of three reaction wheels. However, the Europa orbiter is intended to have a fourth wheel (powered off) which is to be used as a backup in case of any single wheel failure. This gives rise to a more complex orientation problem which must take into account the orientation of the fourth wheel so as to meet requirements in each of the three failed configurations. Such a problem will be considered as part of a future study.

ACKNOWLEDGEMENTS

The author would like to thank Audrey Mark of JPL for technical discussions and system engineering details concerning the Europa mission. This work was supported by the Jet Propulsion Laboratory, California Institute of Technology, under contract with the National Aeronautics and Space Administration.

References

[1] R. Bellman, *Introduction to Matrix Analysis.* Society for Industrial and Applied Mathematics (SIAM), Philadelphia, 1995.

[2] D.P. Bertsekas, *Dynamic Programming and Optimal Control: Volume I.* Athena Scientific, Belmont, Massachusetts, 1995.

[3] Birkhoff, "Tres observaciones sobre el algebra lineal," Rev. univ. nac. Tucuman, ser. A, vol. 5, pp. 147-151, 1946.

[4] D.B. DeBra and R.H. Cannon, "Momentum vector considerations in wheel-jet satellite control system design," *Guidance and Control,* "Progress in Astronautics and Rocketry", vol. 8, edited by R.E. Roberson and J.S. Farrior, AIAA, New York, pp. 565-598, January 1962.

[5] A.W. Fleming and A. Ramos, "Precision three-axis attitude control via skewed reaction wheel momentum management," Proc. AIAA Guidance, Navigation and Control Conference, (Boulder, CO), pp. 177-190, August 1979.

[6] P.E. Gill, W. Murray and M.H. Wright, *Practical Optimization.* Academic Press, Inc., New York, 1981.

[7] G.H. Golub and C.F. Van Loan, *Matrix Computations.* Second Edition, John Hopkins University Press, Baltimore, 1989.

[8] H.B. Hablani, "Sun-tracking commands and reaction wheel sizing with configuration optimization," J. Guidance, Control and Dynamics, Vol. 17, No. 4, pp. 805-814, July-August 1994.

[9] D.L. Russel, *Mathematics of Finite-Dimensional Control Systems.* Marcel Dekker Inc., New York, 1979.

A APPENDIX A: Details Behind Step 1 of Algorithm

This appendix discusses Step 1 of the algorithm in Section 5.2 where the cost $C(b, R, \widehat{Q})$ in (5.5)(5.8) is optimized with respect to b and R using Sequential Quadratic Programming (SQP).

From (5.2), $R \in \mathcal{R}^{3\times 3}$ has the form of an upper triangular matrix with unit norm columns. As discussed in Section 5.1, the matrix R will be parametrized by the vector of parameters $r = [r_1, r_2, r_3]^T \in \mathcal{R}^3$ as follows,

$$R(r) = \begin{bmatrix} 1 & r_1 & r_3 \\ 0 & (1-r_1^2)^{\frac{1}{2}} & r_2(1-r_3^2)^{\frac{1}{2}} \\ 0 & 0 & (1-r_2^2)^{\frac{1}{2}}(1-r_3^2)^{\frac{1}{2}} \end{bmatrix} \tag{A.1}$$

subject to the linear constraints,

$$-1 \leq r \leq 1 \tag{A.2}$$

where as before we have defined,

$$1 \triangleq \begin{bmatrix} 1 \\ 1 \\ 1 \end{bmatrix} \tag{A.3}$$

By inspection, the cost $C(b, R, Q)$ in (5.5) can be factorized as,

$$C(b, R, Q) = y(b, r)^T y(b, r) \tag{A.4}$$

where the vector $y \in \mathcal{R}^{6n+3}$ is given by,

$$y(b, r) = \begin{bmatrix} \frac{1}{c} b \\ \frac{1}{c}(b + R^{-1}Q^T h^*(1)) \\ \vdots \\ \frac{1}{c}(b + R^{-1}Q^T h^*(n)) \\ \frac{1}{\gamma} R^{-1}Q^T \tau^*(1) \\ \vdots \\ \frac{1}{\gamma} R^{-1}Q^T \tau^*(n) \end{bmatrix} \tag{A.5}$$

The vector y is linear in b but nonlinear in r (i.e., through R^{-1}), and the dependence of y on Q has been dropped for notational simplicity. In order to develop an SQP approach, it will be necessary to expand $y(b, r)$ in a Taylor expansion. The expansion of $y(b, r)$ requires derivatives of the quantity,

$$R^{-1}Q^T x \tag{A.6}$$

where the vector $x \in \mathcal{R}^3$ is considered arbitrary for now. Expanding (A.6) to first order with respect to the perturbation $r = \widehat{r} + \delta r$ gives,

$$R^{-1}Q^T x \;=\; \widehat{R}^{-1}Q^T x + \sum_{i=1}^{3} \left.\frac{dR^{-1}}{dr_i}\right|_{r=\widehat{r}} Q^T x \delta r_i \tag{A.7}$$

$$= \hat{R}^{-1}Q^T x - \sum_{i=1}^{3} \hat{R}^{-1}\frac{dR}{dr_i}\bigg|_{r=\hat{r}} \hat{R}^{-1}Q^T x\delta r_i \tag{A.8}$$

$$= \hat{R}^{-1}Q^T x - \sum_{i=1}^{3} \hat{R}^{-1}\mathcal{S}_i(\hat{r})\hat{R}^{-1}Q^T x\delta r_i \tag{A.9}$$

$$= \hat{R}^{-1}Q^T x - H(\hat{r},x)\delta r \tag{A.10}$$

where we have defined,

$$\hat{R}^{-1} \triangleq R^{-1}(r)\Big|_{r=\hat{r}}; \quad \delta r = \begin{bmatrix} \delta r_1 \\ \delta r_2 \\ \delta r_3 \end{bmatrix} \tag{A.11}$$

$$H(\hat{r},x) \triangleq [\hat{R}^{-1}\mathcal{S}_1(\hat{r})\hat{R}^{-1}Q^T x \mid \hat{R}^{-1}\mathcal{S}_2(\hat{r})\hat{R}^{-1}Q^T x \mid \hat{R}^{-1}\mathcal{S}_3(\hat{r})\hat{R}^{-1}Q^T x] \tag{A.12}$$

and where the sensitivity matrices $\mathcal{S}_i,\ i = 1,2,3$ used in (A.9) are defined as,

$$\mathcal{S}_1(r) \triangleq \frac{dR}{dr_1} = \begin{bmatrix} 0 & 1 & 0 \\ 0 & -r_1(1-r_1^2)^{-\frac{1}{2}} & 0 \\ 0 & 0 & 0 \end{bmatrix} \tag{A.13}$$

$$\mathcal{S}_2(r) \triangleq \frac{dR}{dr_2} = \begin{bmatrix} 0 & 0 & 0 \\ 0 & 0 & (1-r_3^2)^{\frac{1}{2}} \\ 0 & 0 & -r_2(1-r_2^2)^{-\frac{1}{2}}(1-r_3^2)^{\frac{1}{2}} \end{bmatrix} \tag{A.14}$$

$$\mathcal{S}_3(r) \triangleq \frac{dR}{dr_3} = \begin{bmatrix} 0 & 0 & 1 \\ 0 & 0 & -r_2 r_3(1-r_3^2)^{-\frac{1}{2}} \\ 0 & 0 & -r_3(1-r_2^2)^{\frac{1}{2}}(1-r_3^2)^{-\frac{1}{2}} \end{bmatrix} \tag{A.15}$$

Expanding $y(b,r)$ in (A.5) to first order about $b = 0,\ r = \hat{r}$ and making use of (A.10) gives,

$$y(b,r) \simeq n(\hat{r}) + M(\hat{r}) \begin{bmatrix} b \\ \delta r \end{bmatrix} \tag{A.16}$$

where,

$$M(\hat{r}) \triangleq \left[\frac{\partial y}{\partial b}, \frac{\partial y}{\partial r}\right] = \begin{bmatrix} \frac{1}{c}I_{3\times 3} & 0 \\ \frac{1}{c}I_{3\times 3} & -\frac{1}{c}H(\hat{r},h^*(1)) \\ \vdots & \vdots \\ \frac{1}{c}I_{3\times 3} & -\frac{1}{c}H(\hat{r},h^*(n)) \\ 0 & -\frac{1}{\gamma}H(\hat{r},\tau^*(1)) \\ \vdots & \vdots \\ 0 & -\frac{1}{\gamma}H(\hat{r},\tau^*(n)) \end{bmatrix} \tag{A.17}$$

$$n(\hat{r}) \triangleq y(0,\hat{r}) = \begin{bmatrix} 0 \\ \frac{1}{c}\hat{R}^{-1}Q^T h^*(1) \\ \vdots \\ \frac{1}{c}\hat{R}^{-1}Q^T h^*(n) \\ \frac{1}{\gamma}\hat{R}^{-1}Q^T \tau^*(1) \\ \vdots \\ \frac{1}{\gamma}\hat{R}^{-1}Q^T \tau^*(n) \end{bmatrix} \tag{A.18}$$

With these definitions, the cost C in (A.4) can be written as,

$$y(b,r)^T y(b,r) \simeq \left(M(\hat{r}_k)\begin{bmatrix} b \\ \delta r \end{bmatrix} + n(\hat{r}_k)\right)^T \left(M(\hat{r}_k)\begin{bmatrix} b \\ \delta r \end{bmatrix} + n(\hat{r}_k)\right) \tag{A.19}$$

Based on this factorization, Step 1 of the algorithm can be broken down into the following sequence of substeps:

DETAILS OF STEP 1

Step 1A: Initialize

$$k = 0 \tag{A.20}$$

$$\hat{r}_k = 0 \tag{A.21}$$

Step 1B: Solve Quadratic Programming Problem

$$\hat{b}_k, \delta\hat{r}_k = \arg\min_{b_k, \delta r_k} \left(M(\hat{r}_k)\begin{bmatrix} b \\ \delta r_k \end{bmatrix} + n(\hat{r}_k)\right)^T \left(M(\hat{r}_k)\begin{bmatrix} b \\ \delta r_k \end{bmatrix} + n(\hat{r}_k)\right) \tag{A.22}$$

subject to the linear constraints,

$$-1 - \hat{r}_k \leq \delta r_k \leq 1 - \hat{r}_k \tag{A.23}$$

Step 1C: Relinearize

$$\hat{r}_{k+1} = \hat{r}_k + \delta\hat{r}_k \tag{A.24}$$

$$k \leftarrow k + 1 \tag{A.25}$$

Go back to Step 1B and repeat until solution converges.

Step 1B defines a quadratic programming (QP) problem which is readily solved (globally) with available software. The problem is then relinearized in Step 1C and an new QP is solved. This sequence of quadratic subproblems defines the SQP approach [6].

A strict step size limit of $\pm\overline{q}_k$ on δr_k can be enforced by the use of additional constraints in the QP,

$$-\overline{q}_k \mathit{1} \leq \delta r_k \leq \overline{q}_k \mathit{1} \tag{A.26}$$

A simple rule for adjusting $\overline{q}_k$ is to reduce it by 5 percent each time the cost increment in successive iterations changes sign, i.e.,

$$\text{if } sign(C_{k-1} - C_{k-2}) \neq sign(C_k - C_{k-1}) \text{ then } \overline{q}_{k+1} = .95\ \overline{q}_k \tag{A.27}$$

where C_k denotes the QP cost at iteration k. This reduces the step size when the cost starts to oscillate between two values (found to be a common steady-state condition for this SQP iteration). More elaborate step size control methods are also possible rcitegillmw, but were not found necessary in this study.

As defined in Step 1A above, the initial condition $\hat{r}_k = 0$ starts the SQP from scratch each time. However, some computation can be saved by replacing this initial condition with the best solution found from the previous Step 1 call, i.e., by continuing to iterate r_k where it left off previously. This modification was used in the final implementation of the algorithm.

B APPENDIX B: Details Behind Step 3 of Algorithm

This appendix discusses Step 3 of the algorithm in Section 5.2 where the cost $C(\widehat{R}^{-1}Q^T b^*, \widehat{R}, Q)$ in (5.5) is optimized with respect to the orthogonal matrix Q. The cost in Step 3 in conveniently put into the following form,

$$C(\widehat{R}^{-1}Q^T\widehat{b}^*, \widehat{R}, Q) = ||YQ^TX||_f^2 \tag{B.1}$$

where,

$$X = [\frac{\widehat{b}^*}{c}, \frac{\widehat{b}^* + \Delta h^*(1)}{c}, ..., \frac{\widehat{b}^* + \Delta h^*(n)}{c}, \frac{\tau^*(1)}{\gamma}, ..., \frac{\tau^*(n)}{\gamma}] \tag{B.2}$$

$$Y = \widehat{R}^{-1} \tag{B.3}$$

Here, $||M||_f$ denotes the Frobenious norm of a given matrix M [7],

$$||M||_f = Tr\{M^TM\}^{\frac{1}{2}} \tag{B.4}$$

and corresponds simply to the sum of squares of the elements of M. The optimization of (B.1) over choice of Q can then be solved analytically using the following result.

THEOREM B.1 (Frobenious Norm Optimization) *Let $X \in \mathcal{R}^{m\times n}$, $Y \in \mathcal{R}^{\ell\times m}$ be arbitrary but non-zero matrices. Consider the following cost function involving the Frobenious norm,*

$$C(Q) = ||YQ^TX||_f^2 = Tr\{X^TQY^TYQ^TX\} \tag{B.5}$$

where the matrix $Q \in \mathcal{R}^{m\times m}$ is constrained to be orthogonal, i.e.,

$$Q^T = Q^{-1} \tag{B.6}$$

Let P_x and P_y be orthogonal matrices obtained from the following eigenvector decompositions,

$$Y^TY = P_y\Lambda_yP_y^T \tag{B.7}$$

$$XX^T = P_x\Lambda_xP_x^T \tag{B.8}$$

$$\Lambda_x = diag\{\lambda_{x1}, ..., \lambda_{xm}\} \tag{B.9}$$

$$\Lambda_y = diag\{\lambda_{y1}, ..., \lambda_{ym}\} \tag{B.10}$$

where the eigenvalues in Λ_x and Λ_y are each assumed to be ordered in a monotonically non-increasing sequence, i.e.,

$$\lambda_{x1} \geq \lambda_{x2} \geq ... \geq \lambda_{xm} \geq 0 \tag{B.11}$$

$$\lambda_{y1} \geq \lambda_{y2} \geq ... \geq \lambda_{ym} \geq 0 \tag{B.12}$$

Then a choice of Q which globally maximizes $C(Q)$ is given by,

$$\overline{Q} = P_x P_y^T \tag{B.13}$$

and a choice of Q which globally minimizes $C(Q)$ is given by,

$$\underline{Q} = P_x J P_y^T \tag{B.14}$$

where J is the reverse identity,

$$J \triangleq \begin{bmatrix} 0 & \cdots & 0 & 1 \\ \vdots & & 1 & 0 \\ 0 & & & \vdots \\ 1 & 0 & \cdots & 0 \end{bmatrix} \tag{B.15}$$

■

The proof of Theorem B.1 will require some preliminary definitions and results.

Permutation Matrices [1] A permutation matrix P of order m is an $m \times m$ matrix possessing exactly a single element of value "1" in each row and column, with all other elements zero. There are known to be exactly $m!$ permutation matrices of any given order m. ■

Doubly Stochastic Matrices [1] A square matrix $A \in \mathcal{R}^{m \times m}$ is *doubly stochastic* if its elements $A = \{a_{ij}\}$ satisfy the following conditions,

$$a_{ij} \geq 0 \tag{B.16}$$

$$\sum_{i=1}^{m} a_{ij} = 1; \quad \sum_{j=1}^{m} a_{ij} = 1 \tag{B.17}$$

■

Birkhoff's Theorem [1][3] Any doubly stochastic matrix $A \in \mathcal{R}^{m \times m}$ can be written as a convex combination of permutation matrices, i.e.,

$$A = \sum_{k=1}^{m!} w_k P_k \tag{B.18}$$

$$w_k \geq 0; \quad \sum_{k=1}^{m!} w_k = 1 \tag{B.19}$$

where $\{P_k\}$, $k = 1, ..., m!$ denotes the set of permutation matrices of order m. ■

Hardy's Theorem [2] Let $\{b_1, ..., b_m\}$ and $\{c_1, ..., c_m\}$ be monotonically nonincreasing sequences of numbers. Associate with each $i = 1, ..., m$ a distinct index j to define the mapping

between indices $j(i)$. Then the sum-of-products cost $\sum_{i=1}^{m} b_i c_{j(i)}$ is maximized when $j(i) = i$ for all i, and minimized when $j(i) = m - i + 1$ for all i. ■

It is necessary to first prove the following result.

LEMMA B.1 (Bounds on an inner product) *Consider vectors $b = [b_1, ..., b_m]^T$ and $[c_1, ..., c_m]^T$ where $\{b_1, ..., b_m\}$ and $\{c_1, ..., c_m\}$ are monotonically nonincreasing sequences of numbers. Let $A \in \mathcal{R}^{m \times m}$ be a doubly stochastic matrix. Then the inner product $b^T Ac$ can be bounded above and below as follows,*

$$b^T Jc \leq b^T Ac \leq b^T c \tag{B.20}$$

where J is the reverse identity given by (B.15). Furthermore, the lower bound is achieved with equality by choosing $A = J$, and the upper bound is achieved with equality by choosing $A = I$. ■

Proof: Using Birkhoff's Theorem (B.18)(B.19), the matrix A in the expression $b^T Ac$ can be replaced by the convex combination of permutation matrices (B.18) to give,

$$b^T Ac = \sum_{k=1}^{m!} w_k b^T P_k c \tag{B.21}$$

Without loss of generality, we can define the first two permutation matrices as,

$$P_1 = I; \quad P_2 = J \tag{B.22}$$

It is noted that each inner-product term $b^T P_k c$ appearing in the summation of (B.21) can be interpreted as a sum-of-products of elements of b with elements of c, as reordered by multiplication with the permutation matrix P_k. Accordingly, by Hardy's theorem, the largest of the terms $\{b^T P_k c\}_{k=1}^{m!}$ is given by using the identity permutation $P_k = P_1 = I$. Hence, an upper bound on the convex combination (B.21) is found by putting all of the weight into the first term (i.e. $w_1 = 1, w_i = 0 \; for \; i \neq 1$) to give,

$$b^T Ac = \sum_{k=1}^{m!} w_k b^T P_k c \leq b^T P_1 c = b^T c \tag{B.23}$$

This establishes the upper bound in (B.20). Note that this upper bound is achieved with equality when $A = I$.

Similarly, by Hardy's theorem, the smallest of the inner-product terms $\{b^T P_k c\}_{k=1}^{m!}$ is given by using the reverse-ordering permutation $P_k = P_2 = J$. Hence, a lower bound on the convex combination (B.21) is found by putting all of the weight into the second term (i.e. $w_2 = 1, \; w_i = 0 \; for \; i \neq 2$) to give,

$$b^T Ac = \sum_{k=1}^{m!} w_k b^T P_k c \geq b^T P_2 c = b^T Jc \tag{B.24}$$

This establishes the lower bound in (B.20). Note that this lower bound is achieved with equality when $A = J$. ■

At this point Theorem B.1 can be proved. The basic idea is to first show that the cost $C(Q)$ has the special inner product form $b^T Ac$, as treated in Lemma B.1. Second, it is shown that the upper and lower bounds on the cost ensured by result (B.20) of Lemma B.1, are achieved with equality for the optimal choices of Q given by (B.13) and (B.14) of Theorem B.1. As desired, this implies that they are in fact global extrema.

Proof of Theorem B.1: Define the cost function as,

$$C(Q) = ||YQ^T X||_f^2 = Tr\{X^T Q Y^T Y Q^T X\} \tag{B.25}$$

Rearranging using the eigenvalue decompositions (B.7)(B.8) and standard trace identities gives,

$$\begin{aligned}
C(Q) &= Tr\{QY^T Y Q^T X X^T\} && \text{(B.26)}\\
&= Tr\{QP_y \Lambda_y P_y^T Q^T P_x \Lambda_x P_x^T\} && \text{(B.27)}\\
&= Tr\{\Lambda_y P_y^T Q^T P_x \Lambda_x P_x^T Q P_y\} && \text{(B.28)}\\
&= Tr\{\Lambda_y L^T \Lambda_x L\} && \text{(B.29)}\\
&= Tr\{\Lambda_y^{\frac{1}{2}} \Lambda_y^{\frac{1}{2}} L^T \Lambda_x^{\frac{1}{2}} \Lambda_x^{\frac{1}{2}} L\} && \text{(B.30)}\\
&= Tr\{\Lambda_y^{\frac{1}{2}} L^T \Lambda_x^{\frac{1}{2}} \Lambda_x^{\frac{1}{2}} L \Lambda_y^{\frac{1}{2}}\} && \text{(B.31)}\\
&= ||\Lambda_x^{\frac{1}{2}} L \Lambda_y^{\frac{1}{2}}||_f^2 && \text{(B.32)}\\
&= \sum_{i=1}^m \sum_{j=1}^m \left(\lambda_{xi}^{\frac{1}{2}} \lambda_{yj}^{\frac{1}{2}} \ell_{ij}\right)^2 = \sum_{i=1}^m \sum_{j=1}^m \lambda_{xi} \lambda_{yj} \ell_{ij}^2 && \text{(B.33)}\\
&= \lambda_x^T A \lambda_y && \text{(B.34)}
\end{aligned}$$

where the following quantities have been defined,

$$L \triangleq P_x^T Q P_y = \{\ell_{ij}\} \tag{B.35}$$

$$\lambda_x = [\lambda_{x1}, ..., \lambda_{xm}]^T \in \mathcal{R}^m \tag{B.36}$$

$$\lambda_y = [\lambda_{y1}, ..., \lambda_{ym}]^T \in \mathcal{R}^m \tag{B.37}$$

$$A = L \otimes L = \{a_{ij} = \ell_{ij}^2\} \tag{B.38}$$

Equation (B.29) follows from (B.28) by the definition of the orthogonal matrix L in (B.35); equation (B.33) follows from the fact that a squared Frobenious norm of a matrix is the sum-of-squares its elements; and equation (B.34) follows by vectorizing equation (B.33), where

the symbol $\otimes$ denotes the Hadamard product (i.e., the element-by-element multiplication of two matrices).

Since L is an orthogonal matrix (i.e., $L^T L = LL^T = I$) each of its rows and columns have unit norm so that the matrix A in (B.38) is doubly stochastic. In addition, the elements of vectors λ_x, λ_y are ordered from highest to lowest, so that the result (B.20) of Lemma B.1 can be applied to the inner product (B.34) to give,

$$\lambda_x^T J \lambda_y \leq C(Q) \leq \lambda_x^T \lambda_y \tag{B.39}$$

The lower bound in (B.39) is achieved with equality by the choice $A = J$, which using (B.38) gives

$$L = J^{\frac{1}{2}} \tag{B.40}$$

where $J^{\frac{1}{2}}$ denotes any Hadamard square root of the matrix J (i.e., any $J^{\frac{1}{2}}$ such that $J = J^{\frac{1}{2}} \otimes J^{\frac{1}{2}}$). Substituting (B.40) into (B.35), and solving for Q gives the global minimum as,

Global Minimum

$$\underline{Q} = P_x J^{\frac{1}{2}} P_y^T \tag{B.41}$$

For simplicity one can choose (non-uniquely) $J^{\frac{1}{2}} = J$ which gives (B.14) as desired. However, $J^{\frac{1}{2}}$ can alternatively be chosen as one of 2^m possible Hadamard roots of J formed by changing the sign on any combination of 1's in J. Any one of these choices gives a alternative global maximum.

The upper bound in (B.39) is achieved with equality with the choice $A = I$ which using (B.38) gives,

$$L = I^{\frac{1}{2}} \tag{B.42}$$

where $I^{\frac{1}{2}}$ denotes any Hadamard square root of the identity matrix I. Substituting (B.42) into (B.35) and solving for Q gives the global maximum as,

Global Maximum

$$\overline{Q} = P_x I^{\frac{1}{2}} P_y^T \tag{B.43}$$

For simplicity one can choose (non-uniquely) $I^{\frac{1}{2}} = I$ which gives (B.13) as desired. However, $I^{\frac{1}{2}}$ can alternatively be chosen as one of 2^m possible Hadamard roots of I formed by changing the sign on any combination of 1's in the identity I. Any one of these choices gives an alternative global maximum. ■

C APPENDIX C: Alternate Derivation of Optimal Q

This appendix gives an alternate derivation of the formulas for the optimal $\overline{Q}$ and $\underline{Q}$ in equations (B.13)(B.14) of Theorem B.1. The derivation is restricted to Q of dimension 3×3, and is included only for pedagogical reasons, since it gave the author his first insights into the problem at hand. The derivation is simple and requires only familiar concepts from calculus which optimize a cost by taking a derivative and setting it equal to zero. However, it would be wrong to interpret this derivation as an alternative proof of the claims in Theorem B.1, which treats Q of arbitrary size and addresses deeper properties related to global optimality.

Define the cost function as,

$$C(Q) = Tr\{X^T Q Y^T Y Q^T X\} \tag{C.1}$$

Let the orthogonal matrix Q be written as a small perturbation to the orthogonal matrix Q_0 as follows,

$$Q = Q_0 + \epsilon \delta Q \triangleq (I - \epsilon \theta^\times) Q_0 \tag{C.2}$$

where we have defined,

$$\delta Q \triangleq -\theta^\times Q_0 \tag{C.3}$$

$$\theta = \begin{bmatrix} \theta_x \\ \theta_y \\ \theta_z \end{bmatrix}; \quad \theta^\times \triangleq \begin{bmatrix} 0 & -\theta_z & \theta_y \\ \theta_z & 0 & -\theta_x \\ -\theta_y & \theta_x & 0 \end{bmatrix} \tag{C.4}$$

Note that the skew-symmetry of the small perturbation $\epsilon\theta^\times$ in (C.2) ensures that Q will be orthogonal if Q_0 is. Define the gradient of C with respect to the orthogonal matrix Q in the direction δQ, evaluated at Q_0 as,

$$C_Q(Q_0) \triangleq \lim_{\epsilon \to 0} \frac{dC(Q_0 + \epsilon \delta Q)}{d\epsilon} \tag{C.5}$$

Evaluating $C(Q_0 + \epsilon \delta Q)$ gives,

$$\begin{aligned} C(Q_0 + \epsilon \delta Q) &= Tr\{X^T (I - \epsilon\theta^\times) Q_0 Y^T Y Q_0^T (I + \epsilon \theta^\times) X\} && \text{(C.6)} \\ &= Tr\{X^T Q_0 Y^T Y Q_0^T X\} && \text{(C.7)} \\ &+ \epsilon Tr\{X^T Q_0 Y^T Y Q_0^T \theta^\times X\} - \epsilon Tr\{X^T \theta^\times Q_0 Y^T Y Q_0^T X\} && \text{(C.8)} \\ &- \epsilon^2 Tr\{X^T \theta^\times Q_0 Y^T Y Q_0^T \theta^\times X\} && \text{(C.9)} \end{aligned}$$

Differentiating and taking the limit gives,

$$\begin{aligned} C_Q(Q_0) &= \lim_{\epsilon \to 0} \frac{dC(Q_0 + \epsilon \delta Q)}{d\epsilon} && \text{(C.10)} \\ &= Tr\{X^T Q_0 Y^T Y Q_0^T \theta^\times X\} - Tr\{X^T \theta^\times Q_0 Y^T Y Q_0^T X\} && \text{(C.11)} \\ &= Tr\{\theta^\times \left(X X^T Q_0 Y^T Y Q_0^T - Q_0 Y^T Y Q_0^T X X^T \right)\} && \text{(C.12)} \end{aligned}$$

A necessary condition for a local extremum is found by setting the gradient (C.12) to zero (cf., [9]) to give,

$$Tr\{\theta^{\times}G\} = 0 \quad \text{for all } \theta \in \mathcal{R}^3 \tag{C.13}$$

where,

$$G = XX^TQ_0Y^TYQ_0^T - Q_0Y^TYQ_0^TXX^T \tag{C.14}$$

As a necessary condition for a local extremum, it is desired for (C.13) to be true for all choices of the perturbation direction $\theta^{\times}$. Since both $\theta^{\times}$ and G are skew-symmetric (i.e., $(\theta^{\times})^T = -\theta^{\times}$ and $G = -G^T$) the choice $\theta^{\times} = G^T$ is valid. With this choice, the necessary condition (C.13) becomes,

$$Tr\{\theta^{\times}G\} = Tr\{G^TG\} = 0 \tag{C.15}$$

which is true if and only if

$$G = 0 \tag{C.16}$$

Hence (C.16) is an equivalent necessary condition for a local extremum.

Let Q_0 be chosen as,

$$Q_0 = P_xP_y^T \tag{C.17}$$

Then one can verify that Q_0 is a local extremum by substituting (C.17) into G and verifying that the necessary condition (C.16) holds. Specifically,

$$\begin{aligned}
G &= XX^TQ_0Y^TYQ_0^T - Q_0Y^TYQ_0^TXX^T && \text{(C.18)}\\
&= P_x\Lambda_xP_x^TQ_0P_y\Lambda_yP_y^TQ_0^T - Q_0P_y\Lambda_yP_y^TQ_0^TP_x\Lambda_xP_x^T && \text{(C.19)}\\
&= P_x\Lambda_xP_x^T(P_xP_y^T)P_y\Lambda_yP_y^T(P_yP_x^T) - (P_xP_y^T)P_y\Lambda_yP_y^T(P_yP_x^T)P_x\Lambda_xP_x^T && \text{(C.20)}\\
&= P_x\Lambda_x\Lambda_yP_x^T - P_x\Lambda_y\Lambda_xP_x^T = 0 && \text{(C.21)}
\end{aligned}$$

Here the last step follows from the fact that $\Lambda_x\Lambda_y = \Lambda_y\Lambda_x$ since they are all diagonal matrices. Accordingly, Q_0 in (C.17) is a local extremum for the problem. The cost associated with this local extremum is calculated as,

$$\begin{aligned}
C(Q_0) &= Tr\{X^TQ_0Y^TYQ_0^TX\} && \text{(C.22)}\\
&= Tr\{Q_0Y^TYQ_0^TXX^T\} && \text{(C.23)}\\
&= Tr\{P_xP_y^TP_y\Lambda_yP_y^TP_yP_x^TP_x\Lambda_xP_x^T\} && \text{(C.24)}\\
&= Tr\{P_x\Lambda_y\Lambda_xP_x^T\} && \text{(C.25)}\\
&= Tr\{\Lambda_y\Lambda_xP_x^TP_x\} && \text{(C.26)}\\
&= Tr\{\Lambda_y\Lambda_x\} && \text{(C.27)}
\end{aligned}$$

Interestingly, the cost in (C.27) depends on how the roots are ordered in Λ_x and Λ_y.

The largest local extremum occurs when the roots are ordered to maximize the cost expression (C.27). A simple method to do this (i.e., by Hardy's theorem) is to order the eigenvalues in both Λ_x and Λ_y from highest to lowest. This is the starting assumption in Theorem B.1 so the optimal Q is given directly by (C.17) which agrees with $\overline{Q}$ in (B.13).

Likewise, the smallest local extremum occurs when the roots are ordered to minimize the cost expression (C.27). A simple method to do this is to order the eigenvalues in Λ_x from highest to lowest, and the eigenvalues of Λ_y from lowest to highest. Because the starting assumption in Theorem B.1 orders the roots of Λ_y from highest to lowest, they must be flipped around to give a minimizing cost. This gives the additional factor of J seen in the formula (B.13) for $\underline{Q}$, compared to (C.17) above.